MATERIALS RESEARCH SOCIETY
SYMPOSIUM PROCEEDINGS

VOLUME 298

Silicon-Based Optoelectronic Materials

EDITORS
M.A. Tischler
R.T. Collins
M.L.W. Thewalt
G. Abstreiter

MRS

MATERIALS RESEARCH SOCIETY SYMPOSIUM PROCEEDINGS VOLUME 298

Silicon-Based Optoelectronic Materials

Symposium held April 12–14, 1993, San Francisco, California, U.S.A.

EDITORS:

M.A. Tischler
ATM
Danbury, Connecticut, U.S.A.

R.T. Collins
IBM T.J. Watson Research Center
Yorktown Heights, New York, U.S.A.

M.L.W. Thewalt
Simon Fraser University
Burnaby, British Columbia

G. Abstreiter
Walter Schottky Institut
Technische Universität München
Garching, Germany

MRS
MATERIALS RESEARCH SOCIETY
Pittsburgh, Pennsylvania

Materials Research Society Symposium B, San Francisco, CA, April 12-14, 1993

LUMINESCENCE PROCESSES IN $Si_{1-x}Ge_x$/Si HETEROSTRUCTURES GROWN BY CHEMICAL VAPOR DEPOSITION

J.C. STURM, X. XIAO AND Q. MI
Department of Electrical Engineering, Princeton Center for Photonic & Optoelectronic Materials (POEM), Princeton University, Princeton, NJ 08544

L.C. LENCHYSHYN AND M.L.W. THEWALT
Department of Physics, Simon Fraser University, Burnaby, B.C. V5A1S6 Canada

ABSTRACT

Well-resolved band-edge exciton photoluminescence (PL) has been observed in strained $Si_{1-x}Ge_x$ heterostructures grown on Si(100) by rapid thermal chemical vapor deposition. The luminescence is due to shallow-impurity bound excitons at low temperatures (under 20K) and at higher temperatures is due to free excitons or electron-hole plasmas, depending on the pump power. The luminescence can also be electrically pumped, with both the electroluminescence and PL persisting above room temperature in samples with a sufficient bandgap offset. Loss of carrier confinement and subsequent non-radiative recombination outside the $Si_{1-x}Ge_x$ is found to be the reason for reduced PL and EL at high temperature.

I. INTRODUCTION

Strained $Si_{1-x}Ge_x$ layers commensurate on Si(100) substrates have been under intense investigation for nearly a decade for the development of silicon-based heterojunction electronic devices, and more speculatively, light emitting devices. While photoluminescence spectra from such $Si_{1-x}Ge_x$/Si structures and Si_mGe_n short period superlattices have been reported for some time [1-3], the interpretation of these initial results has been controversial [4] because of the broad features, emission energies well below expected bandgaps, and correlation of the emission peaks in some work with those of known dislocation luminescence in Si. Well resolved luminescence features of band-edge exciton recombination has been observed only in the last three years; first in thick strained layers with only 4% Ge ($x = 0.04$) [5] and then finally in strained layer quantum wells and superlattices with higher amounts of Ge [6].

The samples in this last work (Ref. 6) were grown by Rapid Thermal Chemical Vapor Deposition (RTCVD), not molecular beam epitaxy (MBE) as in all of the previous work. This paper first reviews the basic RTCVD technique, and then focuses on three separate issues: the basic features and mechanisms of the luminescence in such strained $Si_{1-x}Ge_x$/Si heterostructures grown by RTCVD, electroluminescence, and finally the temperature dependence of the photo- and electroluminescence.

II. RAPID THERMAL CHEMICAL VAPOR DEPOSITION

A schematic diagram of the reactor used for RTCVD is shown in Fig. 1. A single four-inch Si wafer is suspended on quartz pins without a susceptor inside a 175-mm diameter quartz tube, outside of which is a bank of tungsten halogen lamps which heat the wafer. Process gases (typically dichlorosilane, germane, diborane and phosphine in a hydrogen carrier) are introduced into one end of the reactor and removed from the other end by a simple mechanical rotary vane pump. The chamber is not ultra-high vacuum (UHV), and no pump down with a

high vacuum pump is done after loading samples. However, due to the use of a load lock to prevent atmospheric contamination when loading samples, $Si_{1-x}Ge_x$ layers with low oxygen concentrations ($< 10^{18}cm^{-3}$) and high lifetime ($\geq 1\mu s$) can be routinely achieved at a growth temperature of 625 ° C [7]. Although layers have been grown from 500 ° C to 1200 ° C, typical growth conditions (used for all work in this paper unless otherwise specified) are 625 ° C for $Si_{1-x}Ge_x$ growth and 700 ° C for Si. Typical growth rates under these conditions are ~ 100 Å /min. The lack of a susceptor allows fast changes (> 100 K/s) in sample temperature so that the growth temperature of each layer or interface can be optimized. The lack of a susceptor or any other hardware (except for the quartz support pins) also removes possible sources of contamination (e.g. metallic impurities, non-radiative centers, etc.) from the chamber to the maximum degree possible. This is important since the luminescence can easily be quenched by excessive non-radiative recombination. The wafer temperature is monitored *in-situ* during growth with an accuracy of a few K by the measurement of the infrared absorption in the wafer (at 1.3 μm and 1.5 μm), without any adjustable parameters such as emissivity [8]. Further growth details can be found in Ref. 9.

III. PHOTOLUMINESCENCE SPECTRA

Figure 2 shows the typical PL spectra of a single strained 33Å $Si_{0.8}Ge_{0.2}$ quantum well and of a single 500Å $Si_{0.8}Ge_{0.2}$ well (both with $\sim$ 150Å silicon caps) at 2K and 77K. The 2K spectra are qualitatively similar to each other except for a blue shift due to quantum confinement in the narrow QW [10]. They are also similar to those observed by Weber and Alonso in their study of bulk (unstrained) $Si_{1-x}Ge_x$ alloys [11], which allows straightforward interpretation of the features. The highest energy feature results from no-phonon (NP) recombination mediated by the alloy randomness. That the feature exists similarly in both the narrow and wide wells and at 2K and 77K supports the hypothesis that this feature is not due to spatial confinement or low temperature localization effects but is indeed an intrinsic feature of the alloy. The lower energy features are phonon replicas, i.e. from transitions assisted by the emission of momentum-conserving transverse acoustic (TA) and transverse optical (TO) phonons. In the

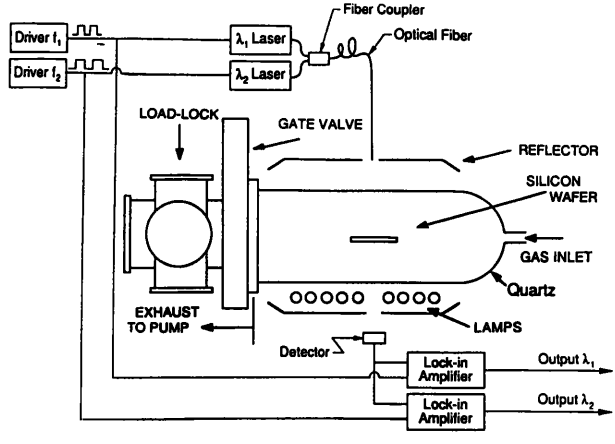

Fig. 1: Schematic cross-section of the RTCVD reactor with temperature measurement by infrared transmission.

33Å well, the narrow linewidth allows one to observe the splitting of the TO replica into various local vibrational modes (Si-Si, Si-Ge, Ge-Ge) representing the different nearest neighbor interactions. From the relative strength of the local modes one can infer the sample composition as shown in bulk material [11], although this ratio is modified in thin QW's and superlattices [6].

On the basis of its temperature dependence, excitation spectroscopy, and lifetime, luminescence at 2K is attributed to excitons bound to a shallow impurity. The background doping of these samples is typically $\sim 10^{16} cm^{-3}$ and may include B or P depending on the reactor history. At higher temperatures ($>$ 20K), the PL is due to free excitons at low pump powers (as seen in Fig. 2a) and to an electron-hole plasma at higher pump powers [12]. The characteristic feature of this electron-hole plasma is a broadening of the lineshape (especially on the low energy side) as the quasi-fermi levels move into the conduction and valence bands. Samples with similar PL at 77K have also been grown at a temperature of 550 ° C. This indicates that growth temperatures over 600 ° C are not required for observing strong band-edge luminescence features.

IV. ELECTROLUMINESCENCE

In this section electroluminescence (EL) is demonstrated by incorporating $Si_{1-x}Ge_x$ QW's in a lightly doped region between n^+ and p^+ Si layers, which inject electrons and holes respectively in forward bias. In previous EL work in $Si_{1-x}Ge_x$ structures, light emission in one case was reported at 4K in samples grown by MBE, but the emission was well below the bandgap and of uncertain origin [13]. In CVD samples with x = 0.2 QW, clear band-edge EL was seen, but it decreased sharply above 150K and was virtually extinct by 200K [14]. In this work we have grown a n^+-i-p^+ structure with ten $Si_{0.65}Ge_{0.35}$ QW's of width ~50Å in the i-region. 60 μm x 60 μm diodes were fabricated by simple mesa etching with aluminum contacts. Light was observed through a window in the top aluminum contact.

Figure 3 shows the 4K and 77K PL on this sample (from a piece not processed into diodes) as well as the EL spectrum (I = 10 μA) with a heat sink temperature of 80K. At 4K, the resolved NP and TO peaks show clear evidence of the band-edge exciton recombination described earlier. The peak NP energy of 890 meV is somewhat higher than that expected for a bound exciton in strained x = 0.35 (870 meV) [15], but this difference is within the range of expected quantum confinement effects and uncertainty in sample parameters. Although thermally broadened at 77K, the spectra are qualitatively similar, indicating a band-edge recombination mechanism (although no longer bound exciton). The magnitude of the blue shift (~30 meV) is not well understood: ~ 15 meV can be understood as due to the BE to FE transition and the band-filling effects described earlier; the remainder of the shift may be due to unintentional differences in the ten QW's and different wells dominating at different temperatures.

At a heat sink temperature of 80K, the 10 mA (400 Hz modulation, 50% duty cycle) EL (Fig. 3) is qualitatively similar to the 77K PL, although broader, presumably due to poor thermal contact between the sample and heat sink and consequently higher sample temperature. Therefore we infer that the EL mechanism also results from band-edge carrier recombination. At a heat sink temperature of 300K, the EL was still clearly observable with a peak at ~ 930 meV (1.3 μm), corresponding to the NP recombination in the SiGe (Fig. 4). Some emission from the TO replica of the cladding Si layers was also evident (which was much weaker at lower temperatures), but this was estimated to make up less than 10%

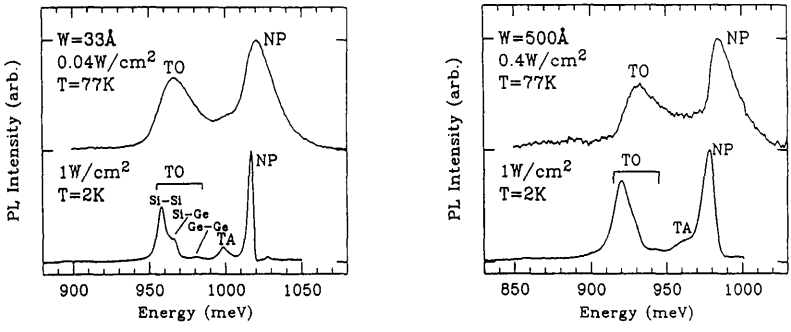

Fig. 2: PL spectra of Si/strained $Si_{1-x}Ge_x$/Si potential wells of width (a) 33Å and (b) 500Å at both 2K and 77K.

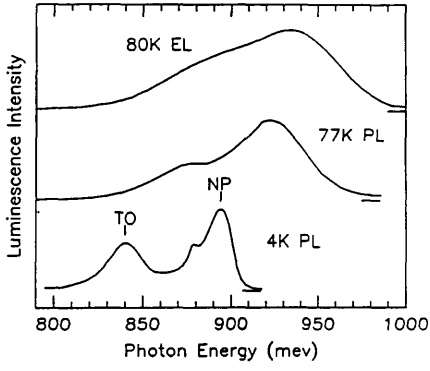

Fig. 3: PL spectra of the EL sample before processing at 4K and 77K, and the EL spectrum with 10 mA drive current and heat sink temperature of 80K.

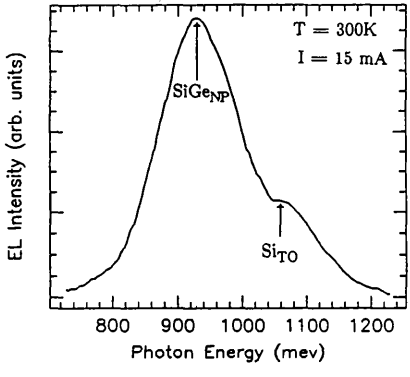

Fig. 4: EL spectra with a drive current of 15 mA at a heat sink temperature of 300K.

of the total amount of emitted light. The peak EL intensity increased linearly with drive current up to 60 mA ($\sim$ 1500 A/cm^2 assuming a uniform current distribution) above an extrapolated threshold of $\sim$ 10 mA (250 A/cm^2), and was sublinear at lower currents (Fig. 5). The weaker emission efficiency at lower drive currents is thought to be due to parasitic space-charge region recombination at defects (such as the mesa sidewalls). At 60 mA, the estimated internal quantum efficiency (after correcting the external signal for window area, solid angle, etc.) had a lower limit of 2 x 10^{-4} [16]. This number is considered a lower limit because of the considerable lateral resistance of the top p^+ layer, so that the current density was probably much higher under the contact area than under the window area.

PL and EL were also studied from a single 10-Å pure Ge layer (grown at 625 ° C) sandwiched between silicon cladding. The microstructure of the Ge layer was not explicitly observed by TEM, etc. The 10Å thickness was estimated from the measured growth rate of Ge from the growth of thick (eg. > 1000Å) Ge layers in other samples, and the Ge layer may be "islanded" and not uniform in thickness. Figure 6 shows the PL (4K and 77K) and EL (90 mA, 80K and 300K heat sink) of such structures. Whereas the room temperature EL peak of the $Si_{0.65}Ge_{0.35}$ QW structure was at 1.3 μm, the room temperature EL peak of the pure Ge structure was at 1.5 μm. The peak intensity at 300K increased linearly above a threshold current density of 25 A/cm^2, but the efficiency at higher drive currents was only $\sim$ 10% that of the 1.3 μm emitter. The physical origin of the EL and PL is not clear, however, due to the very broad spectrum ($\sim$ 100 meV peak) at 4K. It is possible that the origin of the luminescence in this sample is dislocations or other defects and not band-edge carriers.

V. TEMPERATURE DEPENDENCE

Except for the BE to FE transition described in Ref. 6, there is little change in the photoluminescence of most of our $Si_{1-x}Ge_x$ samples from 4K to 77K. Most of the decay in intensity occurs well above 77K. Fig. 7 shows the evolution of the photoluminescence Ar^+-ion excitation ($\sim$ 10 W/cm^2), with increasing temperature above 77K of a single quantum well for both x = 0.2 and x = 0.35. Figure 8 shows the peak intensity of the NP-line in each sample vs temperature. While the x = 0.2 PL decays sharply above 120K and is barely observable at 174K, the x = 0.35 does not decay until temperatures over 200K and is still observable at room temperature. To the best knowledge of the authors, these are the highest temperatures for which PL has been observed in such structures grown by any technique.

A simple quantitative model is now developed to explain what physical mechanism is controlling the decay of PL of higher temperatures. The PL efficiency depends on 3 factors:

$$\eta = \frac{\tau_{\text{non-rad}}}{\tau_{\text{rad}}} \cdot f_{\text{SiGe}} \tag{1}$$

where η is the internal PL efficiency, $\tau_{\text{non-rad}}$ is the non-radiative lifetime

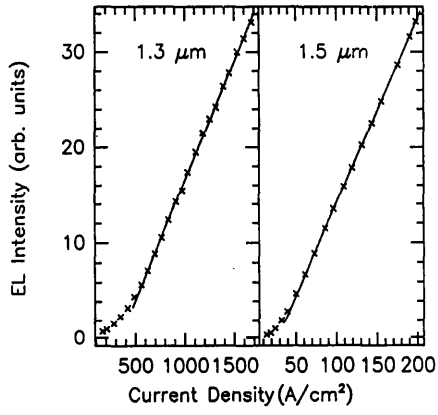

Fig. 5: Peak EL intensity vs. current density (assuming uniform current distribution) of the (a) $Si_{0.65}Ge_{0.35}$ strained QW (1.3 μm) and (b) 10Å pure Ge (1.5 μm) structures. (The vertical axis for the 1.5 μm LED is expanded by ~100 X relative to that for the 1.3 μm LED).

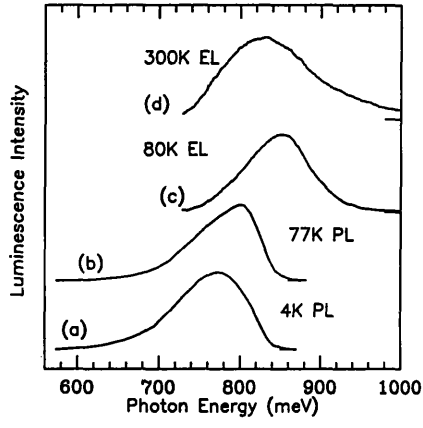

Fig 6. PL (4K and 77K) and EL (90 mA drive current, 80K and 300K heatsink) for the 10-Å Ge layer.

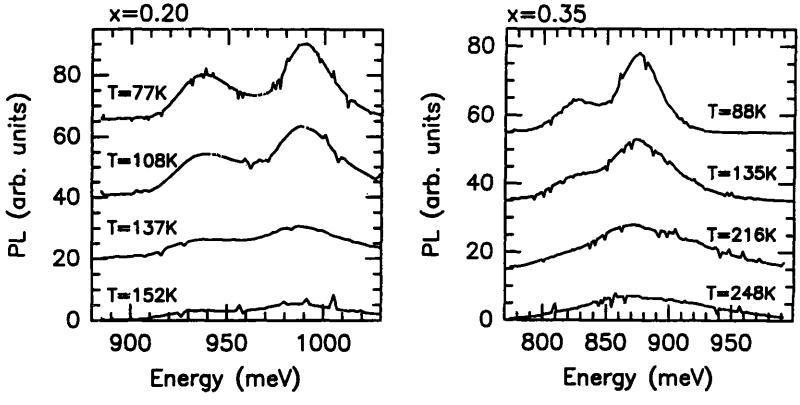

Fig. 7: PL spectra for various temperatures for a single $Si/Si_{1-x}Ge_x/Si$ quantum well with (a) x = 0.2 and (b) x = 0.35.

(assumed much lower than the radiative lifetime), τ_{rad} is the radiative lifetime, and f_{SiGe} is the fraction of carriers in the $Si_{1-x}Ge_x$ well. The radiative lifetime is due to the NP process (due to alloy scattering) and phonon-assisted transitions (predominately TO). For temperatures of 300K or less, these rates are both expected to depend little on temperature because the phonon energies are relatively large (e.g. $\sim$ 670K for the Si TO). At temperatures above 20K, at which carriers are mobile and not localized as bound excitons or otherwise, the dominant nonradiative recombination mechanism is recombination at deep levels, so that the non-radiative lifetime can be described as

$$\tau_{nonrad} = (N_T \sigma v_{th})^{-1} \tag{2}$$

where N_T is the density of levels within the bandgap, σ is their cross-section, and v_{th} the carrier thermal velocity. This lifetime is therefore expected to have only a weak ($\sim T^{-1/2}$) temperature dependence. This apparently leaves f_{SiGe} as the only term which might depend exponentially on the temperature and explain our high temperature luminescence decay.

The fraction of carriers in the SiGe (f_{SiGe}) first depends on the transport of the photo-generated carriers from the Si substrate to the QW. The QW's are within the top 0.05 μm of the sample, while the absorption depth of the pump laser is $\sim 1\mu$m. We have typically observed at 2K that the TO-PL from the Si-substrate is comparable to or stronger than that of the $Si_{1-x}Ge_x$, indicating that only $\leq$ 50% of the generated carriers are collected into the QW before luminescing. By 77K however, the TO-PL from the Si is less than 5% that of the $Si_{1-x}Ge_x$, indicating that nearly all of the carriers are collected by the $Si_{1-x}Ge_x$ [17]. Therefore we can assume that at temperatures over 77K, the redistribution of carriers occurs faster than the luminescence, and that an approximate quasi-equilibrium distribution of carriers is established.

Assuming an equilibrium distribution of carriers (not limited by the transport of carriers to the well) one can describe the carrier populations over the regions of interest by flat quasi-fermi levels and a thermal distribution. Since the valence band offset is much larger than that for holes for strained $Si_{1-x}Ge_x$ on Si, the bandgap offset is most effective on holes, which in turn will attract electrons to the $Si_{1-x}Ge_x$. As a first approximation, the fraction of carriers in the $Si_{1-x}Ge_x$ can then be expressed as

$$f_{SiGe} = \frac{W_{SiGe}}{W_{SiGe} + W_{Si}\, e^{-\Delta E_v/kT}} \tag{3}$$

where W_{SiGe} is the width of the SiGe, W_{Si} is the width of the Si region over which the carriers are distributed, and ΔE_v is the valence band offset. The above neglects any effects of band-bending and also assumes all carrier densities are non-degenerate. For the samples of Fig. 7, $W_{SiGe} = 100\text{Å}$, and W_{Si} can be approximated by a minority carrier diffusion length (estimated at $\sqrt{D\tau} = 10\text{cm}^2/\text{s}\cdot 10^{-6}\text{s} = 3\text{x}10^{-3}\text{cm}$). For x = 0.2, the valence band offset is $\sim$ 160 meV. At 100K and 200K one would then predict $f_{SiGe} \simeq 1.00$ and 0.91, respectively. Clearly, this does not explain the large drop in the $Si_{0.8}Ge_{0.2}$ PL (down by a factor of 100 at 200K). A similar result is found for the x = 0.35 sample.

This inconsistency of the simple model with the data can be resolved by more closely examining the non-radiative lifetime, specifically if one assumes a substantially lower effective lifetime in the Si regions compared to the $Si_{1-x}Ge_x$ layers. This might not result from bulk effects, but could more likely result from a high rate of recombination at the top Si-surface or at the original substrate interface ($\sim 1\ \mu m$ beneath the QW). In this case the overall non-radiative recombination rate for the entire sample can be modelled by an average weighted lifetime, $\tau_{non-rad,avg}$:

$$\tau_{non-rad,avg}^{-1} = \frac{f_{Si}}{\tau_{non-rad,Si}} + \frac{f_{SiGe}}{\tau_{non-rad,SiGe}} \tag{4}$$

$$= \frac{W_{SiGe}}{\tau_{non-rad,SiGe}} \left(\frac{1 + \frac{\tau_{non-rad,SiGe} \cdot W_{Si}}{\tau_{non-rad,Si} \cdot W_{SiGe}} e^{-\Delta E_v/kT}}{W_{SiGe} + W_{Si}\, e^{-\Delta E_v/kT}} \right)$$

where the f_i and $\tau_{non-rad,i}$ are the fraction of carriers and effective lifetime in layer i. Combining this with equations (1) and (3) gives a dominant temperature dependence for the PL as

$$\eta \propto \frac{1}{1 + C \cdot e^{-\Delta E_v/kT}} \tag{5}$$

where

$$C \equiv \frac{\tau_{non-rad,SiGe} \cdot W_{Si}}{\tau_{non-rad,Si} \cdot W_{SiGe}} \tag{6}$$

This expression was fit to the data of the x = 0.2 sample in Fig. 8 using $\Delta Ev = 180meV$ and $C = 5x10^6$, with a reasonably good agreement as shown. That C is much larger than the expected $W_{Si}/W_{SiGe} \simeq 30\mu m/0.01\mu m \simeq 3000$ implies that the effective non-radiative lifetime in the Si is indeed much lower than that in the SiGe. Using the same C, the x = 0.35 data was fit using $\Delta E_v \simeq 310$ meV and again reasonable agreement was achieved (Fig. 7). That the fitted ΔE_v are indeed close to the known ΔE_v values (~180 meV, 270 meV respectively [15]) indicates that the valence band offset is the crucial parameter for the temperature dependence of luminescence. The conclusion of this modeling of the temperature dependence of the PL is that the luminescence decreases at high temperature because of the low effective lifetime for carriers outside the quantum well. Only a relatively few number of carriers are required to be outside of the quantum well to cause a substantial reduction in the luminescence efficiency.

The temperature dependence of the peak SiGe NP electroluminescence signal of our $Si_{0.65}Ge_{0.35}$ QW LED and that of the $Si_{0.8}Ge_{0.2}$ LED of Ref. 14 are shown in Fig. 9 along with the x = 0.2 and x = 0.35 modelling results of Fig. 8. The temperature dependence of the EL is qualitatively similar to that of the PL: sharp decay at high temperatures and higher x (more Ge) resulting in a stronger signal at high temperatures. (The significance of the pronounced feature in the x = 0.35 EL at 190K is not known.) It is clear, however, that the EL does not decay as fast at high temperature as the PL for the same x. This may be due to an extra confining effect of the p-n junction on the injected carriers. Extra confinement could suppress the size of the W_{Si} region or could prevent carriers from reaching the top Si surface. Quantitative modelling to support these effects has not been done however.

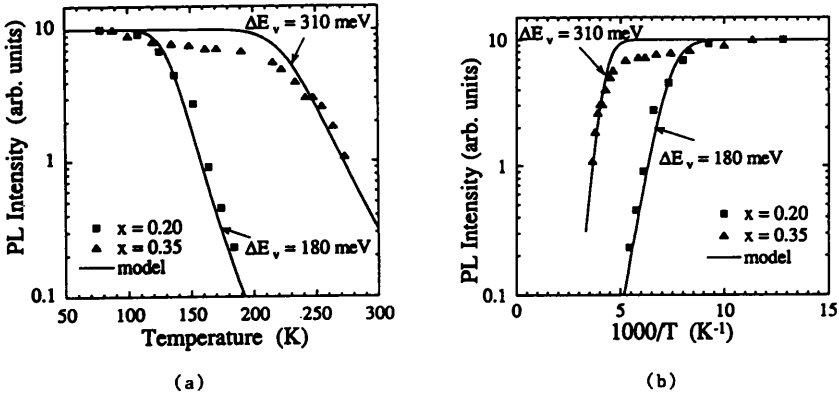

Fig. 8: Peak no phonon photoluminescence intensities vs. (a) temperature and (b) vs. inverse temperature for the x = 0.2 and x = 0.35 QW samples of Fig. 7 and fitted model results are described in the text.

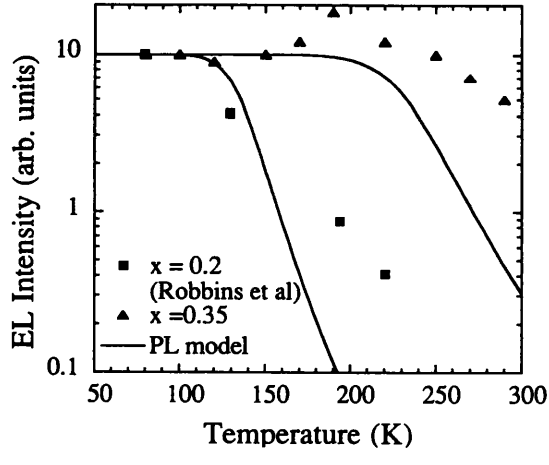

Fig. 9: Peak electroluminescence intensity vs. temperature for the $Si_{0.65}Ge_{0.35}$ QW's and the $Si_{0.8}Ge_{0.2}$ QW's (of Ref. 14), along with the model results for PL vs. temperature of Fig. 8.

VI. SUMMARY

Well resolved exciton luminescence has been observed in Si/strained $Si_{1-x}Ge_x/Si$ quantum well structures grown by Rapid Thermal Chemical Vapor Deposition. Key features are a no-phonon line due to alloy randomness and a threefold splitting of the TO replica. The luminescence process can be pumped electrically as well as optically, with room temperature 1.3μm electroluminescence from the no-phonon process in $Si_{0.65}Ge_{0.35}$ quantum wells. At high temperature the luminescence decreases exponentially with an activation energy close to that of the valence band offset. This decay is thought to be due to excessive recombination in the silicon cladding layers. For x = 0.35, both PL and EL are visible at room temperature, but not at x = 0.2.

VI. ACKNOWLEDGEMENT

The authors would like to thank P.V. Schwartz, C.W. Liu, Z. Matutinovic-Krstelj, A. St. Amour, and V. Venkataraman for experimental assistance and helpful discussions. The support of NSF, ONR, and the New Jersey Commission on Science and Technology (for Princeton) and NSERC (for Simon Fraser University) is gratefully acknowledged.

VII. REFERENCES

1. J.P. Noel, N.L. Rowell, D.C. Houghton and D.D. Perovic, Appl. Phys. Lett. **57**, 1037 (1990).
2. H. Okumura, K. Miki, S. Misawa, K. Sakamoto, T. Sakamoto and S. Yoshida, Jpn. J. Appl. Phys. **28**, L1893 (1989).
3. R. Zachai, K. Eberl, G. Abstreiter, E. Kasper and H. Kibbel, Phys. Rev. Lett. **64**, 1055 (1990).
4. U. Schmid, N.E. Christensen and M. Cardona, Phys. Rev. Lett. **65**, 2610 (1990).
5. K. Terashima, M. Tajima and T. Tatsumi, Appl. Phys. Lett. **57**, 1925 (1990).
6. J.C. Sturm, H. Manoharan, L.C. Lenchyshyn, M.L.W. Thewalt, N.L. Rowell, J.P. Neol, and D.C. Houghton, Phys. Rev. Lett. **66**, 1362 (1991).
7. P.V. Schwartz and J.C. Sturm, Appl. Phys. Lett. **57**, 2004 (1990).
8. J.C. Sturm, P.M. Garone and P.V. Schwartz, J. Appl. Phys. **69**, 542 (1991).
9. J.C. Sturm, P.V. Schwartz, E.J. Prinz and H. Manoharan, J. Vac. Sci. Technol. B**9**, 2011 (1992).
10. X. Xiao, C.W. Liu, J.C. Sturm, L.C. Lenchyshyn and M.L.W. Thewalt, Appl. Phys. Lett. **60**, 2135 (1992).
11. J. Weber and M.I. Alonso, Phys. Rev. B**40**, 5683 (1989).
12. X. Xiao, C.W. Liu, J.C. Sturm, L.C. Lenchyshyn and M.L.W. Thewalt, Appl. Phys. Lett. **60**, 1720 (1992).
13. N.L. Rowell, J.P. Noel, D.C. Houghton and M. Buchana, Appl. Phys. Lett. **58**, 957 (1991).
14. D.J. Robbins, P. Calcott, W.Y. Leong, Appl. Phys. Lett. **59**, 1350 (1991).
15. C.G. van de Walle and R.M. Martin, Phys. Rev. B. **34**, 5621 (1986).
16. Q. Mi, X. Xiao, J.C. Sturm, L.C. Lenchyshyn and M.L.W. Thewalt, Appl. Phys. Lett. **60**, 3177 (1992).
17. J.C. Sturm, X. Xiao, P.V. Schwartz, C.W. Liu, L.C. Lenchyshyn and M.L.W. Thewalt, J. Vac. Sci. Technol. B**10**, 1998 (1992).